# Design Analysis of InN/InGaN Quantum Well Laser with GaN Layers at 1320-1350 nm Wavelength

Md. Mobarak Hossain Polash[*†], *Student Member, IEEE* and M. Shah Alam[*‡], *Senior Member, IEEE*
[*]Department of Electrical and Electronic Engineering
Bangladesh University of Engineering and Technology (BUET)
Dhaka-1000, Bangladesh
[†]Department of EEE, University of Asia Pacific, Bangladesh
[‡]Department of EEE, Northern University Bangladesh (on leave from BUET)
Emails: polash.eee@uap-bd.edu, shalam@eee.buet.ac.bd

***Abstract*— In this work, a nitride based strained single quantum well laser has been designed and characterized at 1330 nm wavelength. Here, InN has been used as well material and InGaN has been used as barrier material along with GaN as separate confinement heterostructure for better carrier and optical confinement. For the analysis of characteristics of the laser system, 6-bands *k . p* formalism for wurtzite semiconductor has been solved considering band mixing effect, strain due to lattice mismatch, spontaneous and piezoelectric polarization and carrier screening effects. The optical gain and spontaneous emission rate and also the interband momentum matrix elements have been calculated to analyze the optical properties of the designed laser and a good agreement with previously published works is obtained.**

***Keywords—optical gain; wurtzite strained semiconductor; k . p method; spontaneous emission rate, interband momentum matrix element.***

## I. INTRODUCTION

Nitride semiconductors have important applications for lasers and light-emitting diodes (LEDs) [1-2], power electronics [3], thermoelectricity [4], solar cells [5], terahertz photonics [6] and high frequency electronic devices [7]. In the last decade, a lot of fundamental and applied research has been done on the wide band gap nitride semiconductors, mainly as materials for lasers and LEDs in the blue-green and ultraviolet spectral regions [1-2]. As nitride lasers and light-emitting diodes (LEDs) have higher lifetimes which make them more commercially attractive over previously used II-VI devices [8]. Recently, nitride based single or multiple quantum wells are also studied in the spectral range over 1100 nm due to the prospect of their applications in optoelectronic devices like waveguide switches, infrared photo-detectors, etc. For modern optical communication, particularly the wavelengths of 1330 nm and 1550 nm are most important for short distance and long distance communication, respectively. At 1330 nm, dispersion of a signal is lowest and at 1550 nm path loss of a signal is the lowest among the available communication wavelength [9]. III-nitride semiconductors like GaN, AlN, InN and their alloys are attracting much interest for optoelectronic devices in these near-infrared spectral range for fiber optic communications.

For designing nitride based semiconductor lasers and LEDs in communication wavelength spectra, generally intersubband (ISB) optoelectronic devices are mostly studied due to the large conduction band offset of the III-nitride heterostructures [10]. For this range, design of interband structures are hardly proposed in recent published works. For attaining the wavelength range, InN is most suitable nitride materials which is mostly proposed as quantum well (QW) material of delta well along with InGaN QWs [11]. In this work, design and analysis have been performed for InN as quantum well material and InGaN as barrier material. Here, GaN has been used as separate confinement heterostructure (SCH). In QW diode laser, SCH is used for better optical confinement as well as carrier confinement in the active region [12]. For the analysis of optical properties including optical gain, spontaneous emission spectrum and interband momentum matrix elements, the calculation of the band structures and wave functions for InN QWs with InGaN barriers and GaN SCH region has been performed by solving the effective mass Hamiltonian based on the six-band ***k . p*** method developed by S. L. Chuang for wurtzite-strained semiconductors [13].

## II. NUMERICAL FORMALISMS OF *K.P* METHOD

For the calculation of the electronic band structure of nitride based system, hole wave functions are calculated based on 6-band ***k . p*** formalism for wurtzite semiconductors [13]. The model takes into account the valence band mixing, strain effect, spontaneous, piezoelectric polarization and the carrier screening effect. Strain is incorporated into the calculation using the deformation potentials [14]. The strain tensor elements in the well region are expressed as [13]:

$$\begin{aligned} \in_{xx} &= \in_{yy} = \frac{a_0 - a}{a}, \\ \in_{zz} &= -\frac{2C_{13}}{C_{33}} \in_{xx}, \\ \in_{xy} &= \in_{yz} = \in_{zx} = 0 \end{aligned} \qquad (1)$$

where, $a_0$ and $a$ are the lattice constants of barrier and well layers respectively. $C_{13}$ and $C_{33}$ are the stiffness constants of the well layer. In this formalisms, the electron energy bands are assumed to be parabolic and the effective mass Hamiltonian can be written as [13]:

$$H^c(\mathrm{k_t}, \mathrm{k_z}) = (\frac{\hbar^2}{2})(\frac{k_t^{\,2}}{m_e^{\,t}} + \frac{k_z^{\,2}}{m_e^{\,z}}) + \mathrm{E_c}^0(\mathrm{z}) + \mathrm{P_{c\in}(z)} \qquad (2)$$

where, the wave vector $\mathrm{k_t} = -i\nabla_t$, $k_z = -i\partial/\partial z$ and $m_e^{\,t}$ and $m_e^{\,z}$ are the electron effective masses perpendicular and

parallel to the growth direction respectively. The hydrostatic energy shift in the conduction band, $P_{c\in}(z)$ is zero in the barrier regions and is non-zero due to a strain in the well region [13]. The spontaneous polarization uses the linear interpolation [15]. Due to polarization, in wurtzite III-nitride semiconductors have a built-in electrostatic fields in each layer which leads to energy band bending. The electrostatic field in *j*th layer as a result of total polarization fields can be expressed as [15]:

$$E_j = \frac{\sum_k l_k P_k / \in_k - P_j \sum_k l_k / \in_k}{\in_j \sum_k l_k / \in_k} \qquad (3)$$

where, $P$ is the total macroscopic polarization, $\square$ is the static dielectric constant and $l$ is the thickness of each layers (*k*th, *j*th). To ensure zero average electric field in the layers, electric field expression in eqn. (3) needs to satisfy the periodic boundary conditions given in [15]. The Hamiltonian for the valence-band structure has been determined using 6×6 diagonalized ***k . p*** Hamiltonian matrix [13],[16]:

$$H_{6\times6}{}^{v}(\mathrm{k}) = \begin{bmatrix} H_{3\times3}{}^{U}(\mathrm{k}) & 0 \\ 0 & H_{3\times3}{}^{L}(\mathrm{k}) \end{bmatrix} \qquad (4)$$

where, $H_{3\times3}{}^{U}$ and $H_{3\times3}{}^{L}$ are 3×3 matrices and are given by

$$H^U = \begin{bmatrix} F & K_t & -iH_t \\ K_t & G & \Delta - iH_t \\ iH_t & \Delta + iH_t & \lambda \end{bmatrix} \qquad (5)$$

$$H^L = \begin{bmatrix} F & K_t & iH_t \\ K_t & G & \Delta + iH_t \\ -iH_t & \Delta - iH_t & \lambda \end{bmatrix} \qquad (6)$$

with the matrix elements as follows

$$F = \Delta_1 + \Delta_2 + \lambda + \theta, \qquad G = \Delta_1 - \Delta_2 + \lambda + \theta$$

$$\lambda = \frac{\hbar^2}{2m_0}(A_1 k_z{}^2 + A_2 k_t{}^2) + D_1 \in_{zz} + D_2(\in_{xx} + \in_{yy})$$

$$\theta = \frac{\hbar^2}{2m_0}(A_3 k_z{}^2 + A_4 k_z{}^2) + D_3 \in_{zz} + D_4(\in_{xx} + \in_{yy}),$$

$$k_t = \frac{\hbar^2}{2m_0} A_5 k_t{}^2, \quad H_t = \frac{\hbar^2}{2m_0} A_6 k_t k_z, \quad \Delta = \sqrt{2}\Delta_3$$

where, the magnitude of the in-plane wave vector can be expressed as $k_t = \sqrt{k_x^2 + k_y^2}$. $\Delta_1$ is the crystal-field split energy and is caused by the anisotropy of the symmetry. $\Delta_2$ and $\Delta_3$ account for the spin-orbit interaction. These parameters has been listed in Table I for GaN, InN and AlN [8],[16-18].

## III. Optical Gain and Spontaneous Emission with Optical Transition Matrix

By using the envelop functions along with electron spin described in [13], the optical interband transition matrix element relating *n*th-state in the conduction band and *m*th-state valence band can be computed by the following relations [13],[16]:

TABLE I. Material Parameters of Nitride Binaries.

| Parameters | GaN | AlN | InN |
|---|---|---|---|
| **Lattice constant (Å)** | | | |
| *a* | 3.189 | 3.112 | 3.545 |
| *c* | 5.815 | 4.982 | 5.703 |
| **Energy Parameters** | | | |
| $E_g$ (eV) at 300 K | 3.437 | 6.00 | 0.6405 |
| $\Delta_1(=\Delta_{cr})$ (eV) | 0.010 | -0.227 | 0.024 |
| $\Delta_2=\Delta_3=\Delta_{so}/3$ | 0.00567 | 0.012 | 0.00167 |
| **Conduction-band effective masses** | | | |
| $m_{//}{}^*/m_0$ at 300 K | 0.21 | 0.32 | 0.07 |
| $m_{\perp}{}^*/m_0$ at 300 K | 0.20 | 0.30 | 0.07 |
| **Valence-band effective mass parameters** | | | |
| $A_1$ | -7.21 | -3.86 | -8.21 |
| $A_2$ | -0.44 | -0.25 | -0.68 |
| $A_3$ | 6.68 | 0.58 | 7.57 |
| $A_4$ | -3.46 | -1.32 | -5.23 |
| $A_5$ | -3.40 | -1.47 | -5.11 |
| $A_6$ | -4.90 | -1.64 | -5.96 |
| **Deformation potentials (eV)** | | | |
| $D_1$ (eV) | -3.6 | -2.9 | -3.6 |
| $D_2$ (eV) | 1.7 | 4.9 | 1.7 |
| $D_3$ (eV) | 5.2 | 9.4 | 5.2 |
| $D_4$ (eV) | -2.7 | -4.0 | -2.7 |
| **Elastic stiffness constants** | | | |
| $C_{11}$ (GPa) | 390 | 396 | 223 |
| $C_{12}$ (GPa) | 145 | 137 | 115 |
| $C_{13}$ (GPa) | 106 | 108 | 92 |
| $C_{33}$ (GPa) | 398 | 373 | 224 |
| **Piezoelectric co-efficients** | | | |
| $d_{13}$ (pmV$^{-1}$) | -1.0 | -2.1 | -3.5 |
| $d_{33}$ (pmV$^{-1}$) | 1.9 | 5.4 | 7.6 |
| **Spontaneous Polarization** | | | |
| $P_{sp}$ (C/m$^2$) | -0.034 | -0.090 | -0.042 |

TE-polarization ($\hat{e} = \hat{x}$ or $\hat{y} \perp c$ axis):

$$\left|\left(M_x\right)_{nm}^{\sigma}(k_t)\right|^2 = \frac{\left|\langle S | p_x | X \rangle\right|^2}{4} \cdot \left\{ \left\langle \phi_n \middle| g_m^{(1)} \right\rangle^2 + \left\langle \phi_n \middle| g_m^{(2)} \right\rangle^2 \right\} \text{ for } \sigma = U$$

$$= \frac{\left|\langle S | p_x | X \rangle\right|^2}{4} \cdot \left\{ \left\langle \phi_n \middle| g_m^{(4)} \right\rangle^2 + \left\langle \phi_n \middle| g_m^{(5)} \right\rangle^2 \right\} \text{ for } \sigma = L \qquad (7)$$

TM-polarization ($\hat{e} = \hat{z} \,||\, c$ axis):

$$\left|\left(M_x\right)_{nm}^{\sigma}(k_t)\right|^2 = \frac{\left|\langle S | p_z | Z \rangle\right|^2}{2} \cdot \left\langle \phi_n \middle| g_m^{(3)} \right\rangle^2 \text{ for } \sigma = U$$

$$= \frac{\left|\langle S | p_z | Z \rangle\right|^2}{2} \cdot \left\langle \phi_n \middle| g_m^{(6)} \right\rangle^2 \text{ for } \sigma = L. \qquad (8)$$

where, $\square_n$ and $g_m$ are conduction and valence band confined states respectively. The upper and lower Hamiltonian blocks are indicated by $\sigma = U$ and $\sigma = L$ respectively. Here, the linewidth broadening time ($\tau_s$) is assumed to have Lorentzian shape with $\tau_s = 0.1$ ps. Based on the Fermi's Golden rule, the

spontaneous emission rate for TE ($e = x$) or TM ($e = z$) polarizations can be obtained by taking into account all interband transitions between $n$th conduction band and $m$th valence subbands as follows [13],[16]:

$$g_{sp}^{e}(\hbar\omega) = \frac{2q^2\pi}{n_r c\varepsilon_0 m_0^2 \omega L_w} \sum_{\sigma=U,L} \sum_{n,m} \int \frac{k_t dk_t}{2\pi} |(M_e)_{\mathrm{nm}}^{\sigma}(k_t)|^2 \cdot \frac{f_n^c(\mathrm{k_t})(1-f_{\sigma m}^{v}(\mathrm{k_t}))(\gamma/\pi)}{(\mathrm{E}_{\sigma,\mathrm{nm}}^{\mathrm{cv}}(\mathrm{k_t})-\hbar\omega)^2+\gamma^2} \quad (9)$$

For the calculation of the spontaneous emission rate, both TE and TM polarizations are taken into account. The total spontaneous emission rate per unit volume per unit energy interval can be written as fellows [13],[16]:

$$r^{spon}(\mathrm{E}=\hbar\omega) = \frac{n_e^2\omega^2}{\pi^2\hbar c^2} \frac{2(2\,\mathrm{g_{sp}}^{x}+\mathrm{g_{sp}}^{z})}{3} \quad (10)$$

In the calculations of the spontaneous emission spectra and optical gain for polar semiconductor, it is necessary to include all possible transitions in the QW region. The polarization field-induced band bending in the III-Nitride QW leads to the breaking of the orthogonality condition. Transitions between such states, which are traditionally 'forbidden' in non-polar semiconductors, may have an appreciable transition probabilities [19].

## IV. Electronic Properties

In this work, 12Å InN quantum well layer has been sandwiched between two 10Å $In_{0.25}Ga_{0.75}N$ barrier layers. At both end of the barrier layer, a separate confinement heterostructure (SCH) of GaN has been used to provide the better confinement for carrier and photon in the active region of the designed laser structure. The successful growth of InN with monolayer precision by molecular beam epitaxy (MBE) has been reported in [20].

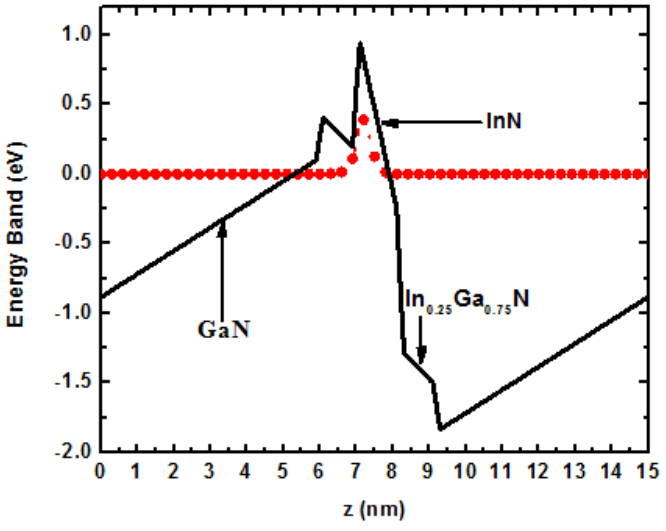


Fig. 1: (Black line) Energy band lineups for valence band of InN (12Å)/ $In_{0.25}Ga_{0.75}N$ (10Å) SQW Laser with electron wave function (red line with circle symbole).

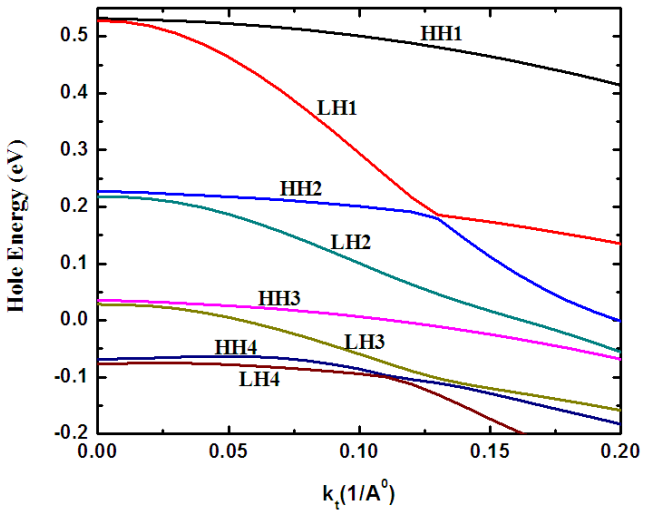


Fig. 2: Valence band structure for $In_{0.25}Ga_{0.75}N$/InN SQW material system along with GaN SCH.

Fig. 1 shows the designed laser structures against z-axis (device growing length) indicating all regions with respective materials along with the energy band lineup for valence band including the effect of internal electric field due to both spontaneous and piezoelectric polarization. In Fig. 2, the valence subbands (first 8 subbands) have been shown as a function of the in-plane wavenumber $k_t$. In this work, bowing parameter of InGaN for gamma energy band calculation is taken as 1.4 eV [8] and for spontaneous polarization calculation is $-0.037\mathrm{C/m^2}$ [8].

## V. Optical Properties

In Fig. 3, the dispersion relation of the square of the momentum matrix elements for TE-polarization described at eqn. 8, have been shown for the designed laser system.

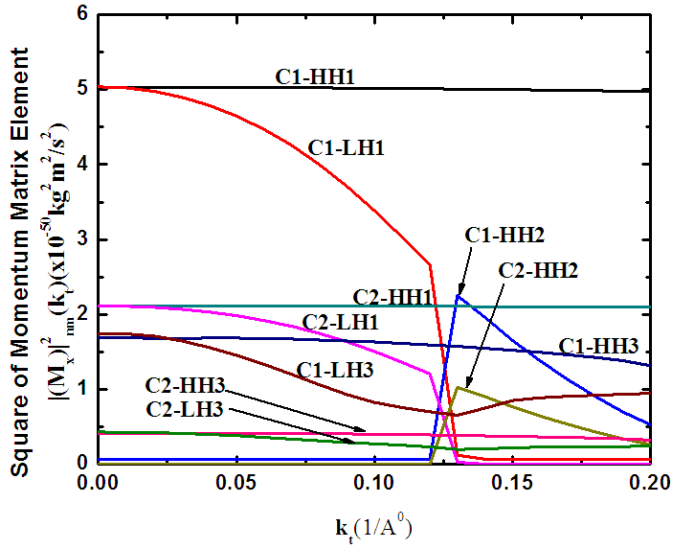


Fig. 3: Square of momentum matrix elements of the TE-polarization for InN(12 Å)/$In_{0.25}Ga_{0.75}N$(10 Å) SQW at carrier density of $5\times10^{19}$ $\mathrm{cm^{-3}}$.

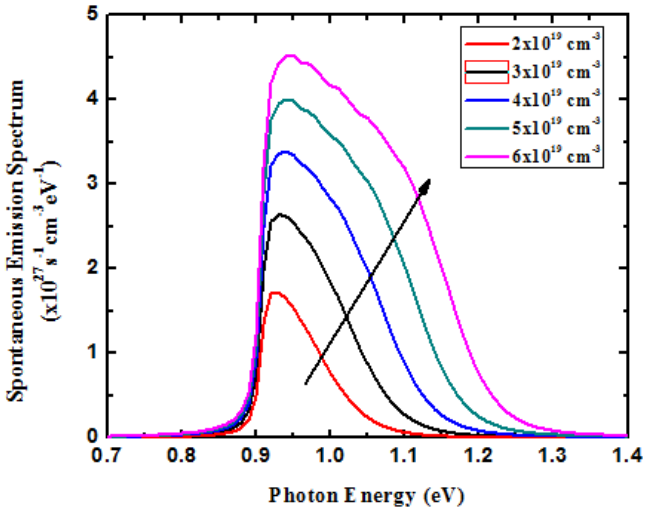


Fig. 4: Spontaneous emission spectra of 12 Å InN SQW laser along with 10 Å barrier of $In_{0.25}Ga_{0.75}N$ for n = $2\times10^{19}$ $cm^{-3}$ to $6\times10^{19}$ $cm^{-3}$ at T=300K.

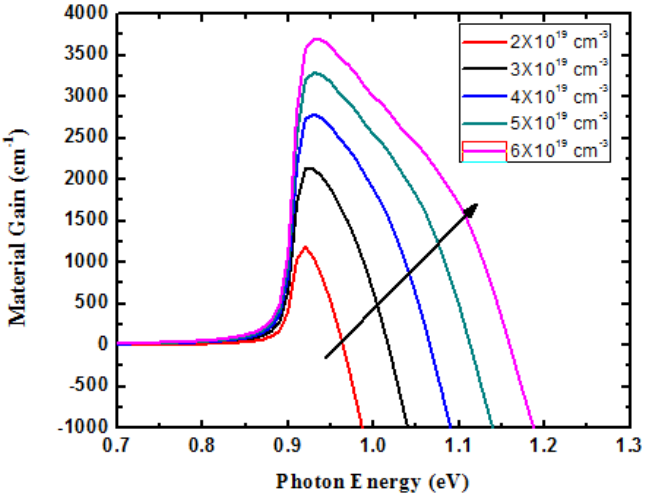


Fig. 5: TE-polarized optical gain spectra of 12 Å InN SQW laser for the carrier density of $2\times10^{19}$ $cm^{-3}$ to $6\times10^{19}$ $cm^{-3}$ at T=300K.

By comparing the transition matrix elements of TE-polarization among the confined state transitions, C1-HH1, C1-LH1, C2-HH1 and C2-LH1 are comparatively strong in spontaneous emission rate contribution for InN/$In_{0.25}Ga_{0.75}N$ SQW laser among the showed momentum matrix elements. Following the eqn. 10, spontaneous emission rate for InN/$In_{0.25}Ga_{0.75}N$ SQW laser has been calculated for several carrier densities ($2\sim6\times10^{19}$ $cm^{-3}$) and the obtained results are shown in Fig. 4. Here it can be that with the increase in carrier density, the peak of the spontaneous emission shows a shift towards lower wavelength due to enhanced carrier screening effect for higher carrier density operation. For carrier density of $2\times10^{19}$ $cm^{-3}$, the peak of the spontaneous emission rate spectra occurs at 1336 nm with an amplitude of $1.72\times10^{27}$ $s^{-1}cm^{-3}eV^{-1}$ and for $6\times10^{19}$ $cm^{-3}$ the peak amplitude of $4\times10^{27}$ $s^{-1}cm^{-3}eV^{-1}$ is found at 1322 nm. In fig. 5, the optical gain spectra for n = $2\times10^{19}$ $cm^{-3}$ up to n = $6\times10^{19}$ $cm^{-3}$ has been shown for designed material system at T=300K using the eqn. 9. Like spontaneous emission rate, as the increase of the carrier density, the peak of the optical gain spectra has been shifted to the shorter wavelength with an enhancement in gain amplitude. This shifting is due to carrier screening effect. From Fig. 5, the peak value of 1190.3 $cm^{-1}$ occurs at 1351.1 nm wavelength for carrier density of $2\times10^{19}$ $cm^{-3}$. For carrier densities $6\times10^{19}$ $cm^{-3}$ the peak wavelength has been found at 1333.7 nm (peak amplitude = 3698.5 $cm^{-1}$) respectively. At carrier density of $4\times10^{19}$ $cm^{-3}$, the peak amplitude of spontaneous emission of $3.38\times10^{27}$ $s^{-1}cm^{-3}eV^{-1}$ is found at 1329.4 nm and peak amplitude of optical gain of 2790 $cm^{-1}$ is found at 1330.8 nm wavelength.

## VI. Conclusion

In this paper, a wurtzite nitride-based single quantum well laser has been designed and analyzed for attaining the wavelength of 1330 nm. Here, 12 Å InN layer has been used as well material along with 10 Å $In_{0.25}Ga_{0.75}N$ layer as barrier material. GaN has been utilized as separate confinement heterostructure (SCH). Several electrical and optical characteristics have been analyzed for the system. Optical transitions between various conduction bands and valence subbands for TE-polarization have been presented. Spontaneous emission rate and optical gain with several carrier densities have been performed for the described system. Due to the carrier screening effect at higher carrier density operation, the peak of both spontaneous emission and optical gain spectra shows a shift towards lower wavelength. The sweeping range of the carrier density is from $2\times10^{19}$ $cm^{-3}$ up to $6\times10^{19}$ $cm^{-3}$. With the increase of carrier density, the peak amplitude of the calculated spontaneous emission and optical gain spectra shows an increase in amplitude. It has been found that, at $2\times10^{19}$ $cm^{-3}$ carrier density, the spontaneous emission spectrum gives peak amplitude of $4\times10^{27}$ $s^{-1}cm^{-3}eV^{-1}$ at 1336.5 nm and the peak optical gain of 1190.3 $cm^{-1}$ occurs at 1351.1 nm. At $6\times10^{19}$ $cm^{-3}$, the spontaneous emission spectrum gives peak amplitude of $1.72\times10^{27}$ $s^{-1}cm^{-3}eV^{-1}$ at 1322 nm and the peak optical gain of 3698.5 $cm^{-1}$ occurs at 1333.7 nm. At $4\times10^{19}$ $cm^{-3}$, the peak amplitude of spontaneous emission spectrum of $3.38\times10^{27}$ $s^{-1}cm^{-3}eV^{-1}$ occurs at 1329.4 nm and the peak optical gain of 2790 $cm^{-1}$ occurs at 1330.8 nm.

## References


[1] D.F. Feezell, M.C. Schmidt, R.M. Farrell, K.C. Kim, M. Saito, K. Fujito, D.A. Cohen, J.S. Speck, S.P. DenBaars and S. Nakamura, "AlGaN-Cladding-Free Nonpolar InGaN/GaN Laser Diodes," *Jpn. J. Appl. Phys.*, vol. 46, pp. L284-286, 2007.

[2] J. Zhang, J. Yang, G. Simin, M. Shatalov, M.A. Khan, M.S. Shur and R. Gaska, "Enhanced Luminescence in InGaN Multiple Quantum Wells with Quaternary AlInGaN Barriers", *Appl. Phys. Lett.*, vol. 77, pp. 2668-2670, Oct. 2000.

[3] U.K. Mishra, P. Parikh and Y.F. Wu, "AlGaN/GaN HEMTs-an Overview of Device Operation and Applications," *Proc. IEEE*, vol. 90, no. 6, pp. 1022-1031, June 2002.

[4] J. Zhang, H. Tong, G.Y. Liu, J.A. Herbsommer, G.S. Huang and N. Tansu, "Characterizations of Seebeck coefficients and thermoelectric

figures of merit for AlInN alloys with various In-contents," *J. Appl. Phys.*, vol. 109, no. 5, 053706-053706-6, Mar. 2011.

[5] M. Jamil, H. Zhao, J.B. Higgins and N. Tansu, "MOVPE and photoluminescene of narrow band gap (0.77eV) InN on GaN/Sapphire by Pulsed Growth Mode,", *Phys. Status Solidi A*, vol. 205, no. 12, pp. 2886-2891, Dec. 2008.

[6] G. Sun, G, Xu, Y.J. Lin, H. Zhao, G. Liu, J. Zhang and N. Tansu, "Efficient Tetrahertz Generation from Multiple InGaN/GaN Quantum Wells," *IEEE J. Sel. Top. Quantum Electron*, vol. 17, no. 1, pp. 48-53, Jan./Feb. 2011.

[7] M.A. Khan, Q. Chen, M.S. Shur, B.T. McDermott, J.A. Higgins, J. Burm, W.J. Schaff and L.F. Eastman, "Microwave Operation of GaN/AlGaN-doped Channel Heterostructure Filed Effect Transistors," *IEEE Electron Device Lett.*, vol. 17, no. 7, pp. 325-327, July 1996.

[8] I. Vurgftman and J.R. Meyer, "Band Parameters for Nitride-containing Semiconductors," *J. Appl. Phys.*, vol. 94 (6), pp. 3675-3696, Sep. 2003.

[9] H.J.R. Dutton, "Understanding Optical Communications," IBM, 1998.

[10] H. Machhadani, P. Kandaswamy, S. Sakr, A. Vardi, A. Wirtmuller, L. Nevou, F. Guillot, G. Pozzovivo, M. Tchernycheva, A. Lupu, L. Vivien, P. Crozat, E. Warde, C. Bougerol, S. Schacham, G. Strasser, G. Bahir, E. Monroy and F.H. Julien, "GaN/AlGaN Intersubband Optoelectronic Devices," *New J. Phys.*, vol. 11 (120523), pp. 1-16, Dec. 2009.

[11] H. Zhao, G. Liu and N. Tansu, "Analysis of InGaN-delta-InN Quantum Wells for Light-emitting Diodes", *Appl. Phys. Lett.*, vol. 97, 131114, 2010.

[12] J. Hecht, "The Laser Guidebook," McGraw-Hill, New York, 1993.

[13] S.L. Chuang, "Optical Gain of Strained Wurtzite GaN Quantum-Well Lasers," *IEEE J. Quantum Electronics*, vol. 32, no. 10, pp. 1791-1800, Oct. 1996.

[14] J. Bardeen and W. Shockley, "Deformation Potentials and Mobilities in Nonpolar Crystals," *Phys. Rev.*, vol. 80, pp. 72-80, 1950.

[15] F. Bernardini and V. Fiorentini, "Spontaneous versus Piezoelectric Polarization in III-V Nitrides: Conveptual Aspects and Practical Consequences," *Phys. Stat. Sol. (b)*, vol. 216, pp. 391-398, Nov. 1999.

[16] H. Zhao, R.A. Arif, Y.K. Ee and N. Tansu, "Self-Consistent Analysis of Strain-Compensated InGaN-AlGaN Quantum Wells for Lasers and Light-Emitting Diodes," *IEEE J. Quantum Electronics*, vol. 45, no. 1, pp. 66-78, Jan. 2009.

[17] J. Piprek, "Nitride Semiconductor Devices: Principles and Simulation," Wiley-VCH, New Jersey, 2007, pp. 24.

[18] J. Piprek, "Semiconductor Optoelectronic Devices: Introduction to Physics and Simulation," Academic Press, San Diego, 2003, pp. 34.

[19] W.W. Chow and M. Kneissl, "Laser Gain Properties of AlGaN Quantum Wells," *J. Appl. Phys.*, vol. 98, Dec. 2005, Art. 114502.

[20] G. Koblmuller, C.S. Gallinat, S. Bernardis, J.S. Speck, G.D. Chern, E.D. Readinger, H. Shen and M. Wraback, "Optimization of the Surface and Structural Quality of N-face InN Grown by Molecular Beam Epitaxy," *Appl. Phys. Lett.*, vol. 89, no. 7, pp. 071902-071902-3, Aug. 2006.